Resonance Raman Spectra of Spinach Ferredoxin and Adrenodoxin and of Analogue Complexes

Vittal K. Yachandra,[†] Jeffrey Hare,[†] Andrew Gewirth,[†] Roman S. Czernuszewicz,[†] T. Kimura,[‡] Richard H. Holm,[§] and Thomas G. Spiro*[‡]

Contribution from the Departments of Chemistry, Princeton University, Princeton, New Jersey 08544, Wayne State University, Detroit, Michigan 48202, and Harvard University, Cambridge, Massachusetts 02138. *Received September 7, 1982*

Abstract: Resonance Raman spectra of oxidized spinach ferredoxin and adrenodoxin show six and seven bands in the Fe-S stretching region (280-430 cm^{-1}). Reconstitution of the proteins with labile ^{34}S using rhodanese and $^{34}SSO_3^{2-}$ produced isotope shifts allowing identification of all four Fe_2S_2 bridging modes and two (three for adrenodoxin) of the four expected Fe-S(Cys) terminal modes. Similar spectra are observed for the analogue complexes $Fe_2S_2(S_2\text{-}o\text{-xyl})_2^{2-}$ (S_2-*o*-xyl = *o*-xylylenedithiolate) and $Fe_2S_2Cl_4^{2-}$, but they show the expected D_{2h} selection rules, and IR-active modes are absent or weak in the Raman spectra. All eight (bridging plus terminal) stretching modes were located via IR as well as Raman spectroscopy and were calculated with reasonable accuracy by using a Urey-Bradley force field scaled to the crystallographically determined interatomic distances. The spinach ferredoxin and $Fe_2S_2(S_2\text{-}o\text{-xyl})_2^{2-}$ frequencies are very similar, but adrenodoxin shows appreciably different terminal frequencies, suggestive of conformational differences of the ligated cysteines. The strong activation of IR modes in the protein Raman spectra implies a protein-induced inequivalence of the two ends of the Fe_2S_2 complex, which may contribute to the known localization of the added electron in the reduced form. This influence is suggested to be due to enhanced H bonding to the cysteine sulfur atoms at one end of the complex, consistent with available crystal structure data. Reduction of adrenodoxin shifts the bridging frequencies 16-24 cm^{-1} to lower frequency, consistent with the expected weakening of the bridging bonds. The terminal modes, however, were unobserved, plausibly due to a loss of enhancement associated with weakened terminal S → Fe charge transfer intensity, except for a weak band at 308 cm^{-1}. At higher frequencies, 550-850 cm^{-1}, the protein spectra showed weak bands associated with the Fe-S overtone and combination levels. Previously reported spin-ladder Raman bands of adrenodoxin and spinach ferredoxin were not observed and are attributed to artifacts produced by laser-induced protein damage. A very broad (~200 cm^{-1}) and weak feature at ~1000 cm^{-1} in the adrenodoxin spectrum might possibly be due to the $S = 0 \rightarrow 1$ electronic transition of the spin-coupled Fe^{3+} ions.

Proteins containing two Fe atoms and two labile S atoms function as one-electron redox components in a wide range of biological electron transfer chains.[1,2] The first to be isolated were ferredoxins from chloroplasts, which are electron carriers on the reducing side of the photosynthetic chain.[3] Another class of 2-Fe proteins is involved in providing electrons to monooxygenase (cytochrome P-450) enzymes, e.g., in the steroid hydroxylation complex of mammalian adrenal gland mitochondria (adrenodoxin)[4] or the camphor hydroxylation complex of the bacterium *Pseudomonas putida* (putidaredoxin).[5] The representatives of these two classes of 2-Fe proteins, while similar in many respects, show differences with respect to their redox potentials,[4,6a] magnetic susceptibility,[6b] EPR,[6c] and MCD[6d] spectra.

The unusual EPR spectrum generated upon reduction drew initial attention to these proteins[7] and led Gibson and co-workers[8] to propose a model involving spin-coupled Fe^{2+} and Fe^{3+} ions, bridged by sulfide ions, with terminal ligands provided by cysteine side chains.[8] The essential features of this model were confirmed and elaborated by extensive spectroscopic characterization,[9] and its validity was firmly established by the synthetic work of Holm and co-workers,[10-13] who succeeded in synthesizing analogues, using the chelating ligand *o*-xylyl dithiolate to prevent further oligomerization of Fe_2S_2 centers. The analogues had essentially the same spectroscopic signatures as the proteins. X-ray crystallography[10,11] showed these complexes to have the expected structure, with tetrahedrally coordinated Fe atoms bridged by S atoms, and gave details of the bond lengths and angles. Only recently has a 2-Fe protein crystal structure begun to emerge.[14] At 2.5 Å the active site shows the Fe atoms bridged by S atoms and coordinated by two cysteine ligands each, as expected.[15]

In this study, we report detailed resonance Raman (RR) spectra of a representative of each of the two main 2-Fe protein classes, ferredoxin from spinach (sp fd) and adrenodoxin (ado). Over the years there have been preliminary reports of RR spectra for these species[16-19] but sufficiently high quality spectra to permit a proper analysis have awaited the development of appropriate experimental techniques, as discussed in the preceding paper.[20] We are now

[†] Princeton University.
[‡] Wayne State University.
[§] Harvard University.

(1) Orme-Johnson, W. H. *Annu. Rev. Biochem.* **1973**, *43*, 159.
(2) Hall, D. O.; Cammack, R.; Rao, K. K. In "Iron in Biochemistry and Medicine"; Jacob, A.; Worwood, M., Eds.; Academic Press: New York, 1974; Chapter 8.
(3) Yocum, C. F.; Siedov, J. N.; Pietro, A. S. In "Iron-Sulfur Proteins"; Lovenberg, W., Ed.; Academic Press: New York, 1973; Vol. I, Chapter 4, p 112.
(4) Estabrook, R. W.; Simpson, K.; Mason, J. I.; Baron, J.; Taylor, W. E.; Simpson, E. R.; Purvis, J.; McCarthy, J. In "Iron-Sulfur Proteins"; Lovenberg, W., Ed.; Academic Press: New York, 1973; Vol. I, Chapter 8, p 193.
(5) Gunsalus, I. C.; Lipscomb, J. D. In "Iron-Sulfur Proteins"; Lovenberg, W., Ed.; Academic Press: New York, 1973; Vol. I, Chapter 6, p 151.
(6) (a) Palmer, G.; Dunham, W. R.; Fee, J. A.; Sands, R. H.; Iizuka, T.; Yonetani, T. *Biochim. Biophys. Acta* **1971**, *245*, 201. (b) Kimura, T.; Tasaki, A.; Watari, H. *J. Biol. Chem.* **1970**, *245*, 4450. (c) Orme-Johnson, W. H.; Sands, R. H. In "Iron-Sulfur Proteins"; Lovenberg, W., Ed.; Academic Press: New York, 1973; Vol. II, Chapter 5, p 195. (d) Thompson, A. J.; Cammack, R.; Hall, D. O.; Rao, K. K.; Briat, B.; Rivoal, J. C.; Badoz, J. *Biochim. Biophys. Acta* **1977**, *493*, 132.
(7) Palmer, G. In "Iron-Sulfur Proteins"; Lovenberg, W., Ed.; Academic Press: New York, 1973; Vol. II, Chapter 8, p 286.
(8) Gibson, J. R.; Hall, D. O.; Thornly, J. M. H.; Whatley, F. R. *Proc. Natl. Acad. Sci. U.S.A.* **1966**, *56*, 987.
(9) Sands, R. H.; Dunham, W. R. *Q. Rev. Biophys.* **1975**, *7*, 443.
(10) Mayerle, J. J.; Denmark, S. E.; DePamphilis, B. V.; Ibers, J. A.; Holm, R. H. *J. Am. Chem. Soc.* **1975**, *97*, 1032.
(11) Mayerle, J. J.; Frankel, R. B.; Holm, R. H.; Ibers, J. A.; Phillips, W. D.; Weiher, J. F. *Proc. Natl. Acad. Sci. U.S.A.* **1973**, *70*, 2429.
(12) Gillum, W. O.; Frankel, R. B.; Fonier, S.; Holm, R. H. *Inorg. Chem.* **1976**, *15*, 1095.
(13) Reynolds, J. G.; Holm, R. H. *Inorg. Chem.* **1980**, *19*, 3257.
(14) Tsukihara, T.; Fukuyama, K.; Tahara, H.; Kaisube, Y.; Matsuura, Y.; Tanaka, N.; Kakudo, M.; Wada, K.; Matsubara, H. *J. Biochem.* (*Tokyo*) **1978**, *84*, 1645.
(15) Fukuyama, K.; Hase, T.; Matsumoto, S.; Tsukihara, T.; Katsube, Y.; Tanaka, N.; Kakudo, M.; Wada, K.; Matsubara, H. *Nature* (*London*) **1980**, *286*, 522.
(16) Tang, S.-P. W.; Spiro, T. G.; Mukai, K.; Kimura, T. *Biochem. Biophys. Res. Commun.* **1973**, *53*, 869.
(17) Yamamoto, T.; Palmer, G.; Ramai, L.; Gill, D.; Salmeen, I. *Fed. Proc., Fed. Am. Soc. Exp. Biol.* **1974**, *33*, 1372.
(18) Adar, F.; Blum, H.; Leigh, J. S., Jr.; Ohnishi, T.; Salerno, J. C.; Kimura, T. *FEBS Lett.* **1977**, *84*, 214.

0002-7863/83/1505-6462$01.50/0

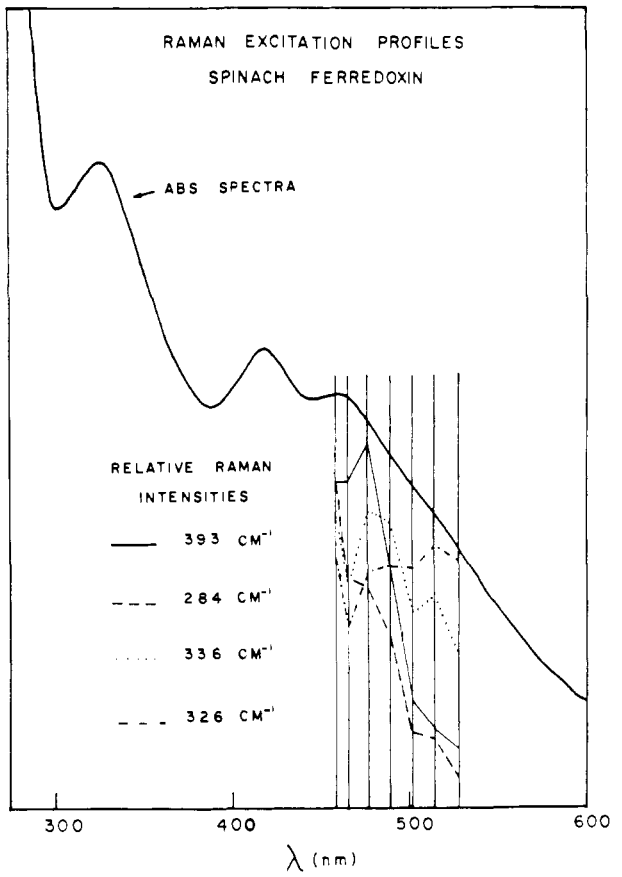

Figure 1. Excitation profiles of bridging and terminal Fe–S modes of oxidized spinach ferredoxin, superimposed on the absorption spectrum. RR band intensities were increased relative to the ν_1 band of SO_4^{2-}, added as an internal standard.

able to make complete assignments of the Fe–S stretching modes, based on isotope shifts observed for ^{34}S-reconstituted protein, together with RR and IR spectra of the analogue complexes $Fe_2S_2(S_2\text{-}o\text{-xyl})_2^{2-}$ (S_2-*o*-xyl = *o*-xylylenedithiolate) and $Fe_2S_2Cl_4^{2-}$, and an approximate normal mode calculation. The sp fd and ado RR spectra show differences that are suggestive of cysteine conformational differences. The striking enhancements of IR active modes in both proteins imply a strong asymmetry in the protein environment, which may contribute to the localization of the added electron in the reduced forms. Reduced adrenodoxin shows lowered bridging mode frequencies, but the terminal Fe–S modes have not been observed. The spin-ladder RR bands reported by Adar et al.[18,19] could not be found. A weak broad band at ~ 1000 cm^{-1} in the ado spectrum may conceivably be due to the $S = 0 \rightarrow 1$ transition.

Materials and Methods

Adrenodoxin was isolated from beef adrenal glands as described elsewhere.[21] Spinach ferredoxin was prepared by the method described in ref 22. The proteins were further purified by Sephadex G-100 gel filtration and by DEAE-52 fractionation. The 422/280 nm absorbance ratio was 0.49 for sp fd while the 414/276 nm ratio was 0.8 for ado. Reduced ado was prepared by the anaerobic addition of a small excess of sodium dithionite.

Both apoproteins were prepared by repeated precipitation with 5% trichloroacetic acid. The labile S content of the apoprotein thus prepared was negligible. ^{34}S was substituted in the Fe_2S_2 site by reconstituting the proteins enzymatically with rhodanese[23,24] isolated from beef liver[25] and

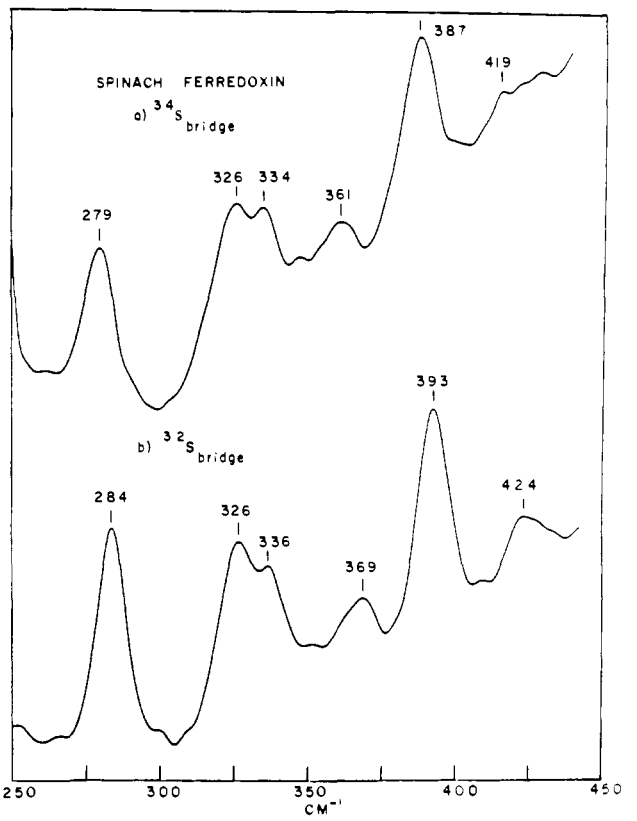

Figure 2. Resonance Raman spectrum of oxidized spinach ferredoxin (1 mM in 0.2 M Tris-HCl buffer, pH 7.6): (a) native protein; (b) reconstituted with ^{34}S. The spectra were collected by backscattering from sealed, spinning, NMR tubes cooled with cold N_2 gas by using 4579-Å Ar^+ laser excitation (200 mW) and a 6-cm^{-1} slit width.

a small amount of ^{34}S-labeled thiosulfate, $^{34}SSO_3^{2-}$, which was prepared by refluxing a stoichiometric amount of elemental ^{34}S (Monsanto) in aqueous Na_2SO_3. A solution was prepared to contain 0.3 mM $Fe(NO_3)_3$, 2 mM dithiothreotol, 1.25 mM $Na_2{}^{34}SSO_3$, and 0.012 mM rhodanese in 0.17 M tris-HCl buffer at pH 7.6. Apoprotein was added to a concentration of 0.125 mM after sufficient time had elapsed to allow for the (100-fold excess of) $^{34}SSO_3^{2-}$ to come to equilibrium with rhodanese.[27-29] The reconstituted protein was separated from the incubation mixture by passing it through a DEAE-52 ion-exchange column and further purified by Sephadex G-100 gel filtration.

$(Et_4N)_2[Fe_2S_2(S_2\text{-}o\text{-xyl})_2]$ and $(Et_4N)_2(Fe_2S_2Cl_4)$ were prepared as described in ref 13 and 30.

Resonance Raman spectra were excited with various lines from Ar^+ and Kr^+ lasers. The protein solutions were placed in sealed spinning NMR tubes and cooled with a stream of cold N_2 gas. Absorption spectra recorded before and after collecting the Raman spectra showed negligible damage due to laser irradiation. Adrenodoxin was reduced anaerobically with a minimum amount of dithionite and reoxidized with no change in either the RR or the absorption spectra. The scattered radiation was collected at an angle of about 45° to the incident beam. The RR spectra of adrenodoxin at liquid N_2 temperature were collected by backscattering off the surface of a frozen protein solution placed in a low-temperature Dewar. The RR spectra of the analogues $[Fe_2S_2(S_2\text{-}o\text{-xyl})_2]^{2-}$ and $(Fe_2S_2Cl_4)^{2-}$ were collected with the tetraethylammonium salts in KBr pellets in a liquid N_2 Dewar by backscattering. The spectrometer consists of a Spex 1401 double monochromator equipped with a cooled RCA 31034 photomultiplier. Spectra were collected digitally by using a MINC II computer and smoothed with a Fourier transform filter, as described in the preceding paper.[20] The peak positions, however, were determined from the unsmoothed data. Weak peaks were accepted as

(19) Blum, H.; Ada, F.; Salerno, J. C.; Leigh, J. S., Jr. *Biochem. Biophys. Res. Commun.* **1977**, *77*, 650.
(20) Yachandra, V.; Hare, J.; Moura, I.; Moura, J. J. G.; Xavier, A. J.; Spiro, T. G. *J. Am. Chem. Soc.*, preceding paper in this issue.
(21) Kimura, T. *Struct. Bonding (Berlin)* **1968**, *5*, 1.
(22) Petering, D. H.; Palmer, G. *Arch. Biochem. Biophys.* **1970**, *141*, 456.
(23) Finazzi, Agro A.; Canella, C.; Graziani, M. T.; Cavallini, D. *FEBS Lett.* **1971**, *16*, 172.
(24) Bonami, F.; Pagani, S.; Cerletti, P. *FEBS Lett.* **1977**, *84*, 149.
(25) Horowitz, P.; DeToma, F. *J. Biol. Chem.* **1970**, *245*, 984.
(26) Anderson, E. B. *Z. Phys. Chem., Abt. B* **1936**, *32*, 237.
(27) Green, J. R.; Westley, J. *J. Biol. Chem.* **1961**, *236*, 3047.
(28) Westley, J.; Nakamoto, T. *J. Biol. Chem.* **1962**, *237*, 547.
(29) Wang, S.-F.; Volini, M. *J. Biol. Chem.* **1968**, *243*, 5465.
(30) Wang, G. B.; Bobrik, M. A.; Holm, R. H. *Inorg. Chem.* **1978**, *17*, 578.
(31) Wilson, E. B.; Decius, J. C.; Cross, P. C. "Molecular Vibrations"; McGraw-Hill: New York, 1955.

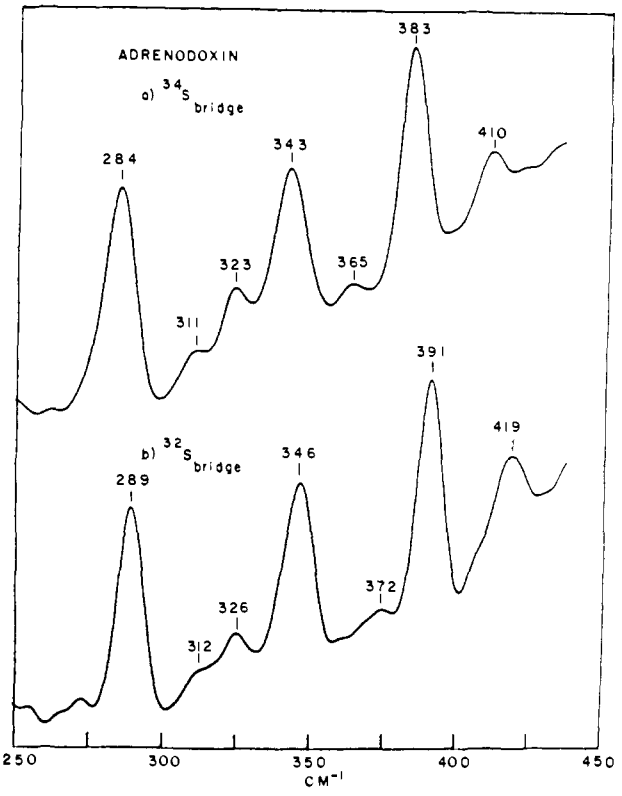

Figure 3. Resonance Raman spectrum of oxidized adrenodoxin (~1 mM in 0.2 M Tris-HCl buffer, pH 7.6): (a) native protein; (b) reconstituted with ^{34}S. Conditions as for Figure 2.

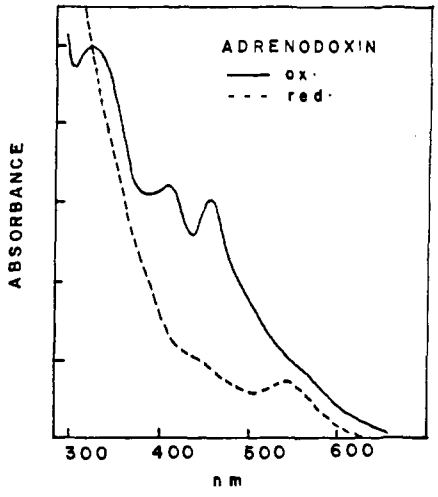

Figure 4. Absorption spectra of oxidized and dithionite-reduced adrenodoxin.

real, if they could be reproduced in separate experiments.

The IR spectra of the analogues $[Fe_2S_2(S_2\text{-}o\text{-}xyl)_2]^{2-}$ and $(Fe_2S_2Cl_4)^{2-}$ were collected with Et_4N^+ salts in Nujol mulls held between polyethylene plates by using a Digilab FTIR instrument.

Results

The Fe_2S_2 proteins and analogue complexes show overlapping absorption bands through the visible region, rising into the near-ultraviolet, which are attributed to S → Fe charge-transfer (CT) transitions.[7,10] Visible laser excitation produces RR spectra whose major bands are found in the 275–425-cm^{-1} region, where Fe–S stretching vibrations are expected. Figure 1 shows the sp fd absorption spectrum, as well as partial excitation profiles for the strongest RR bands. Best RR spectra were obtained with blue excitation (4579, 4545 Å), via backscattering from ~1 mM protein solutions, contained in spinning NMR tubes, cooled with a stream of cold N_2 gas. Figures 2 and 3 show spectra obtained in this way for sp fd and ado and for their ^{34}S reconstituted forms.

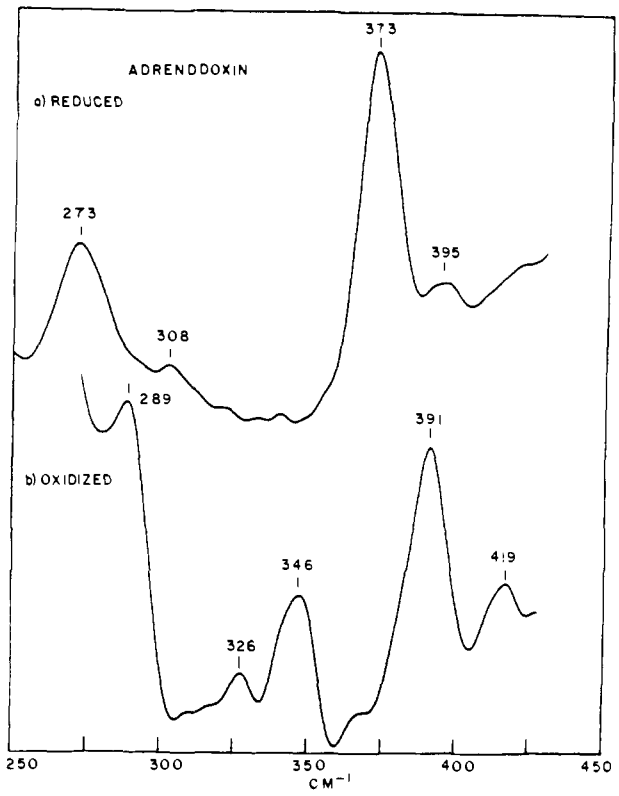

Figure 5. Resonance Raman spectra of adrenodoxin (2 mM, in 0.2 M in 0.2 M) (b) oxidized and (a) reduced (anaerobic dithionite) obtained with 5682-Å Kr^+ laser excitation (200 mW) and a 10-cm^{-1} slit width (backscattering from sealed, spinning NMR tubes cooled with cold N_2 gas).

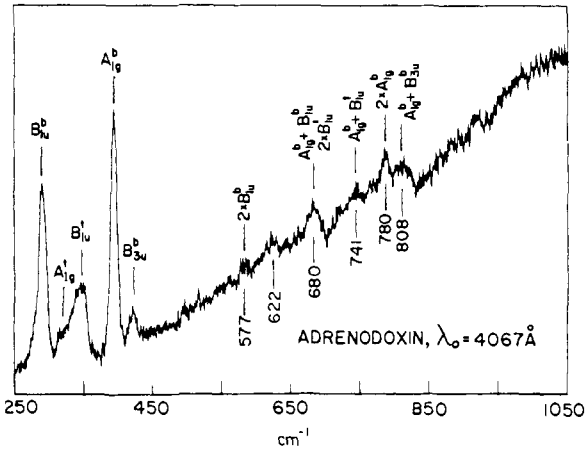

Figure 6. Frozen solution (see ref 45 for details) resonance Raman spectrum of oxidized adrenodoxin, with 4067-Å excitation. Expected positions of the overtones and combinations of the Fe–S stretches are indicated.

The isotope shifts confirm the Fe–S character of these vibrational bands. Reduction of the proteins weakens the visible absorption bands by about half, as shown in Figure 4 for ado. The RR spectrum of reduced ado (ado_{red}) could only be obtained with 5682-Å excitation (Figure 5) in a long-wavelength band in the absorption spectrum, which appears to retain most of the intensity of the ado_{ox} counterpart.

Good quality spectra, with somewhat sharpened features, were also obtained on small amounts (2–3 drops) of protein solution frozen on a liquid N_2 cold tip and excited via backscattering from a Dewar; this method also has the advantage of avoiding background scattering from glass. The Fe-S overtone and combination bands could be identified in these spectra, as shown for adrenodoxin in Figure 6. For the analog complexes, best results were obtained with KBr pellets of their Et_4N^+ salts in a liquid N_2 dewar

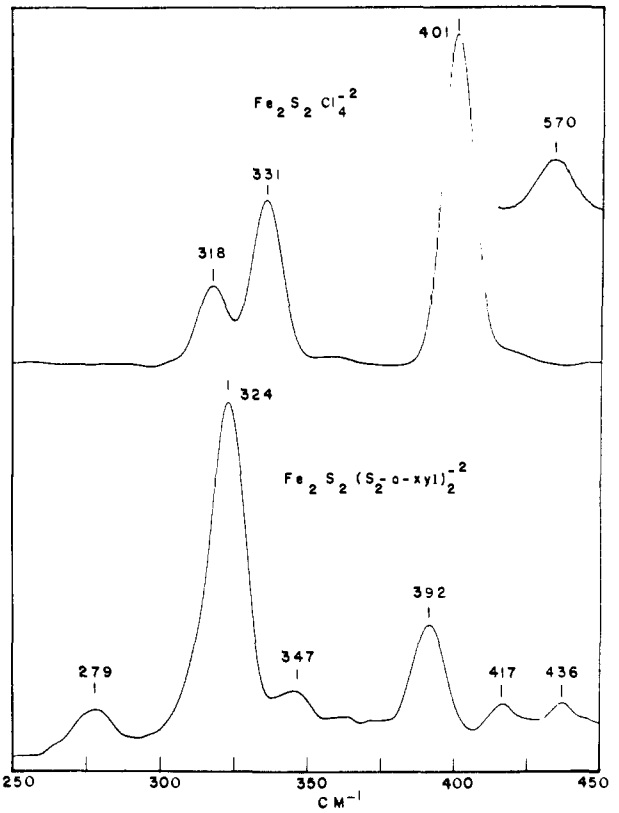

Figure 7. Resonance Raman spectra of $Fe_2S_2(S_2\text{-}o\text{-xyl})_2^{2-}$ and $Fe_2S_2Cl_4^{2-}$, as the Et_4N^+ salts in KBr pellets, obtained in a liquid N_2 Dewar, by backscattering, by using 4545-Å Ar^+ laser excitation (20 mW) and a 10-cm^{-1} slit width.

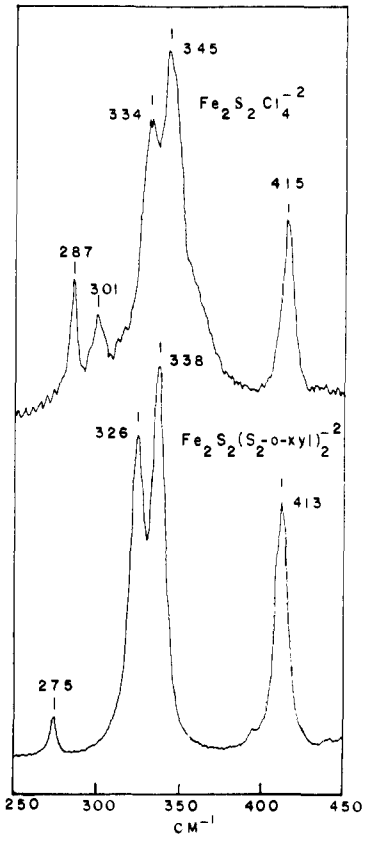

Figure 8. IR spectra of $Fe_2S_2(S_2\text{-}o\text{-xyl})_2^{2-}$ and $Fe_2S_2Cl_4^{2-}$ as Et_4N^+ salts in Nujol mulls, held between polyethylene plates, obtained with a Digilab FTIR spectrometer.

(Figure 7). Infrared spectra were collected for Nujol mulls of the same salts, with a FTIR spectrometer (Figure 8).

Table I. Urey-Bradley Force Constants (mdyn/Å) for a $Fe_2S_2(SCH_2CH_3)_4$ Model, with Structure Parameters from $Fe_2S_2(S_2\text{-}o\text{-xyl})_2^{2-}$

K		*H*		*F*	
$Fe\text{-}S_b$	1.44	$S_b\text{-}Fe\text{-}S_b$	0.25	$S_b\cdots S_b$	0.05
$Fe\text{-}S_t$	1.13	$Fe\text{-}S_b\text{-}Fe$	0.27	$S_t\cdots S_b$	0.09
S-C	2.0	$S_t\text{-}Fe\text{-}S_b$	0.25	$S_t\cdots S_t$	0.08
C-C	2.5	$S_t\text{-}Fe\text{-}S_t$	0.20	$C\cdots Fe$	0.05
Fe-Fe	0.27	C-S-Fe	0.15	$C\cdots S$	0.3
		C-C-S	0.15		

Table II. Fundamental Fe-S (and Fe-Cl) Stretching Modes (cm^{-1}) of Fe_2S_2 Proteins and Analogues

assignment[b]	$Fe_2S_2Cl_4^{2-}$		$Fe_2S_2(S_2\text{-}o\text{-xyl})_2^{2-}$				
	R[c]	IR[c]	R	IR	sp fd, R	ado, R	calcd[a]
B_3u^b		415	417	413	424 (5)[d]	419 (9)[d]	411 (7)[d]
A_1g^b	401		392		393 (6)	391 (8)	398 (6)
B_2g^b			347[e]		369 (8)	372 (7)	345 (5)
B_1u^t		345		338	336 (2)	346 (3)	360 (3)
B_2u^t		334		326			338 (0)
B_3g^t	331		324		326 (0)	312 (1)	338 (0)
A_1g^t	318		~310		~310	326 (3)	310 (3)
B_1u^b		287	279	275	284 (5)	289 (5)	286 (3)

[a] Calculated frequencies by using a Urey-Bradley force field (Table I) for a $Fe_2S_2(S_2CH_2CH_3)_4$ model. The 10 remaining normal modes, largely angle bending in character, are calculated at frequencies below 200 cm^{-1}. [b] Mode symmetry in the idealized D_{2h} point group: superscript b = primarily $Fe\text{-}S_b$ stretching; superscript *t* = primarily $Fe\text{-}S_t$ (or Fe-Cl) stretching. [c] R = observed in Raman spectrum; IR = observed in IR spectrum. [d] $^{34}S_b$ isotope shift (cm^{-1}) in parentheses. [e] Assignment uncertain.

A normal mode calculation was carried out as an aid in assigning the Fe-S vibrations, using the GF matrix method[30] and Schachtschneider's programs[32] for constructing the G matrix and solving the secular equation. To simulate the Fe_2S_2 unit with cysteine ligands, a $Fe_2S_2(SCH_2CH_3)_4$ model was used, with point mass methyl and methylene groups and bond distances and angles from the crystal structure[10] of $(Et_4N)_2[Fe_2S_2(S_2\text{-}o\text{-xyl})_2]$. A Urey-Bradley force field was used, to allow for S···S nonbonded interactions, which are expected to be important. The force constants associated with the CH_3CH_2S Fe units were carried over from the previous study[20] of $Fe(SCH_2CH_3)_4$; the $Fe\text{-}S_4$ stretching constants were adjusted for the slight bond distance difference by using Badger's rule.[33] The bridge stretch and bend force constants, as well as the $S_b\cdots S_b$, $S_b\cdots S_t$ nonbonded constants, were chosen to give a reasonable fit to the clearly identified (via ^{34}S shifts) bridging modes and also to be consistent with the values required in a parallel study[34] of tetrameric $Fe_4S_4(SR)_4^{2-}$ species. Table I lists the force constants used. They include a small Fe-Fe stretching constant, consistent with the short (2.7 Å[10]) Fe-Fe distances. No attempt was made to carry out a least-squares refinement at this stage. The Fe-S-C-C dihedral angles were set at 90°, consistent with the analogue crystal structure, a value known[20] to minimize the $Fe\text{-}S_t$ stretch, S-C-C band interaction. This interaction increases for angles of 0° and 180° and is expected to have differential effects on the different $Fe\text{-}S_t$ modes.[20] These effects were not explored in the present study, although they may account for spectral differences between sp fd and ado (vide infra).

Table II compares the calculated frequencies and ^{34}S shifts with the observed frequencies and assignments for the proteins and analogues.

(32) Schachtschneider, J. H. Shell Development Co., Technical Report No. 263-62, 1962.
(33) Hershbach, D. R.; Laurie, V. W. *J. Chem. Phys.* **1961**, *35*, 458.
(34) Czernuszewicz, R.; Johnson, M. K.; Nelson, H.; Remsen, E.; Hare, J.; Gewirth, A.; Yachandra, V.; Holm, R. H.; Spiro, T. G., manuscript in preparation.
(35) Bobrik, M. A.; Hodgson, K. O.; Holm, R. H. *Inorg. Chem.* **1977**, *16*, 1851.

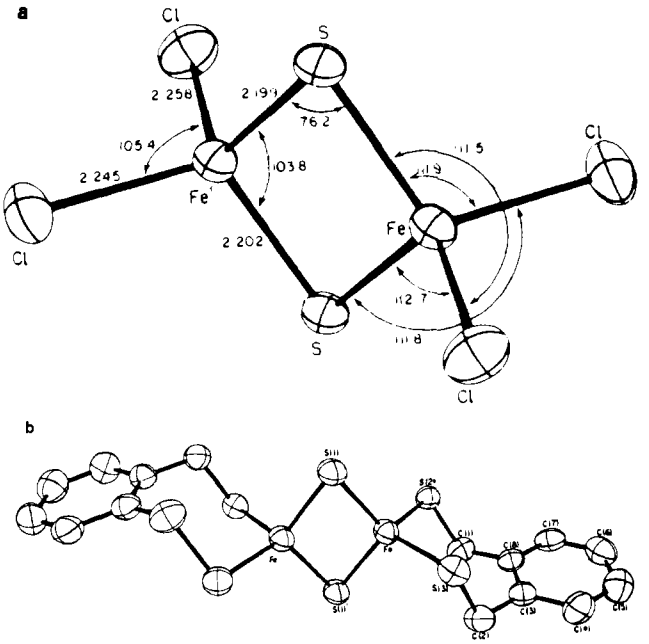

Figure 9. (a) ORTEP diagram of $Fe_2S_2Cl_4^{2-}$ in its Et_4N^+ salt, from ref 35. (b) ORTEP diagram of $Fe_2S_2(S_2\text{-}o\text{-xyl})_2^{2-}$, in its Et_4N^+ salt, from ref 10.

Discussion

Fe–S Assignments. The structure[35] of $Fe_2S_2Cl_4^{2-}$ (Figure 9a) is very close to having ideal D_{2h} symmetry. The inequivalent Fe–S and Fe–Cl terminal bonds differ by only 0.002 and 0.007 Å from the mean values of 2.305 and 2.252 Å, respectively. The structure[10] of $Fe_2S_2(S_2\text{-}o\text{-xyl})_2^{2-}$ (Figure 9b) has only C_2 symmetry, because of the chelated ligands, but the $Fe_2S_2S_4$ portion is nearly isostructural with $Fe_2S_2Cl_4^{2-}$. The Fe–S_b (b = bridging) distances are slightly (0.008 Å) longer on average, while the Fe–S_t (t = terminal) distances are 0.053 Å longer than the Fe–Cl distances. The bond angles are nearly the same. The eight bond stretching modes for a D_{2h} $Fe_2S_2X_4$ structure are illustrated in Figure 10. (The remaining 10 normal modes, involving bending coordinates primarily, are omitted from the discussion since no candidate low-frequency RR bands have been detected.) Normal modes have been assigned and analyzed for the analogous molecules Fe_2Cl_6[36] and Ga_2Cl_6.[37] These differ from $Fe_2S_2Cl_4^{2-}$ in having longer bonds to the bridging atoms and shorter bonds to the terminal atoms (2.28 and 2.11 Å for Fe_2Cl_6); consequently, the actual frequencies differ appreciably from those observed here. Because of the center of symmetry, there should be no Raman–IR coincidences, except accidental ones. For $Fe_2S_2Cl_4^{2-}$ we do observe mutual exclusion, but IR modes show up weakly in the RR spectrum of $Fe(S_2\text{-}o\text{-xyl})_2^{2-}$, reflecting the symmetry lowering by the chelating *o*-xylyl ring, and strongly in the protein RR spectra.

The bridging modes can be identified via their large $^{34}S_b$ isotope shifts in the protein RR spectra. Both sp fd and ado show bands (Figures 2 and 3) near 420, 390, 370, and 285 cm^{-1} that shift 5–8 cm^{-1} on $^{34}S_b$ substitution. (The strong ado bands at 391 and 289 cm^{-1} had previously been identified with bridging modes via their large shifts on Se substitution.[16]) Their frequencies and isotope shifts are in reasonable agreement with the calculated values (Table I). $Fe_2S_2Cl_4^{2-}$ and $Fe_2S_2(S_2\text{-}o\text{-xyl})_2^{2-}$ have IR bands near 415 and 280 cm^{-1} (Figure 8), confirming the B_{3u} and B_{1u} assignments of the highest and lowest frequency bridging modes. Weak RR bands (Figure 7) are seen at the corresponding frequencies for $Fe_2S_2(S_2\text{-}o\text{-xyl})_2^{2-}$ but not of $Fe_2S_2Cl_4^{2-}$ [although a 570-cm^{-1} band does appear and is assigned to the overtone of the 287-cm^{-1} IR frequency, which is Raman active ($2 \times B_{1u} = A_g$)]. Both modes are seen in the protein RR spectra, implying substantial symmetry lowering (vide infra); the B_{1u} mode is especially strong. The A_g bridging mode is readily assigned to the strong RR bands of the analogue complexes, at 401 and 392 cm^{-1}, which correlates with the strong ~390-cm^{-1} protein bands. The fourth bridging mode, seen weakly at ~370 cm^{-1} in the protein RR spectra, is not detected for $Fe_2S_2Cl_4^{2-}$. It is of B_{2g} symmetry and requires vibronic coupling for RR activation,[38] unless the site symmetry is lowered. Assignment of a weak 347-cm^{-1} RR band of $Fe_2S_2(S_2\text{-}o\text{-xyl})_2^{2-}$ to this mode is possible, but uncertain in view of the 20 cm^{-1} downshift relative to the protein frequencies.

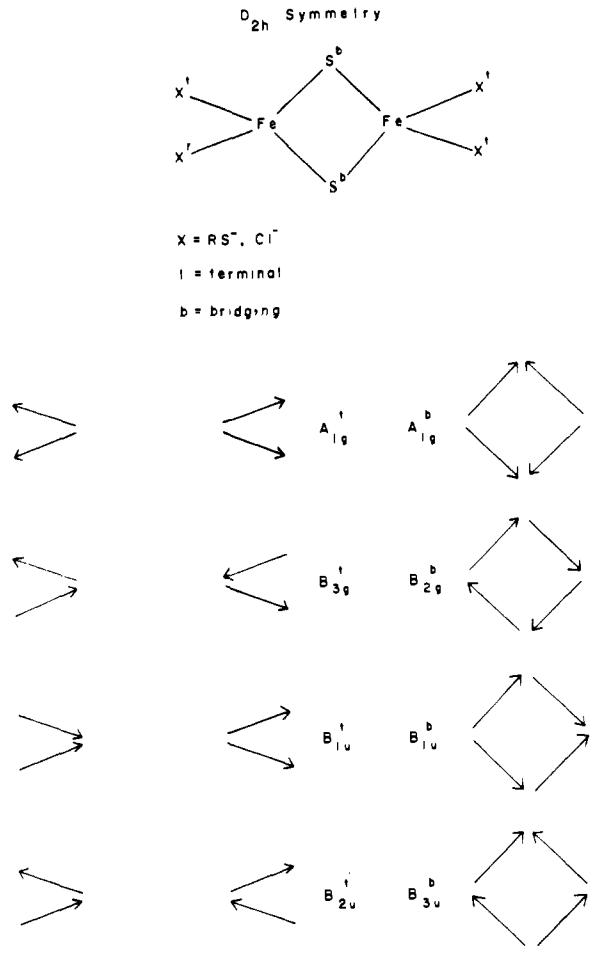

Figure 10. Diagram of the phases of the stretching modes for a D_{2h} $Fe_2S_2X_4$ structure.

The terminal modes cluster in the 310–350-cm^{-1} region, since the kinematic interactions of the terminal bond stretches are smaller than those of the bridge bond stretches. The analogue complexes show a pair of strong IR bands in this region (Figure 8), corresponding to the two expected terminal u modes. The corresponding g modes are seen (Figure 7) as the 318, 331 cm^{-1} pair of RR bands of $Fe_2S_2Cl_4^{2-}$; $Fe_2S_2(S_2\text{-}o\text{-xyl})_2^{2-}$ has a broad 324-cm^{-1} band, with asymmetry on the low-frequency side indicating another band at ~310 cm^{-1}. Specific assignments rest on the expectation that the $B_{2u}{}^t$ and $B_{3g}{}^t$ modes occur at essentially the same frequency, since they differ only in the phasing of the Fe–S_t (or Fe–Cl) stretches on opposite sides of the bridge (Figure 10) and neither mode interacts with any other mode. (An Fe–S_t, Fe–S_t interaction force constant across the bridge would be required to produce a frequency separation.) Consequently, the nearly coincident IR and RR bands, at 334 and 331 cm^{-1} for $Fe_2S_2Cl_4^{2-}$ and at 326 and 324 cm^{-1} for $Fe_2S_2(S_2\text{-}o\text{-xyl})_2^{2-}$, are assigned to $B_{2u}{}^t$ and $B_{3g}{}^t$, respectively. This leaves the remaining IR (345 and 338 cm^{-1}), and RR (318 and ~310 cm^{-1}) bands, assigned to $B_{1u}{}^t$ and $A_g{}^t$, respectively. It is notable that the $A_g{}^t$

(36) Frey, R. A.; Werder, R. D.; Güinthard, H. H. *J. Mol. Spectrosc.* **1970**, *35*, 260.
(37) Adams, D. M.; Churchill, R. G. *J. Chem. Soc. A* **1970**, 697.
(38) Spiro, T. G.; Stein, P. *Annu. Rev. Phys. Chem.* **1977**, *28*, 501.
(39) Spiro, T. G.; Hare, J. W.; Yachandra, V.; Gewirth, A.; Johnson, M. K.; Remsen, E. In "Iron-Sulfur Proteins"; Spiro, T. G., Ed.; Wiley: New York. In Press.

RR bands are less intense than the B_{3g}^t bands, although the latter require vibronic activation[38] (vide infra).

The protein RR spectra differ markedly in the terminal mode region (Figures 2 and 3). Ado shows a strong band at 346 cm^{-1} and weak ones at 326 and 312 cm^{-1}, while sp fd shows strong bands at 336 and 326 cm^{-1}, and the latter has asymmetry on the low-frequency side, suggesting a band at ~310 cm^{-1}. The 336-cm^{-1} sp fd band shows a 2-cm^{-1} $^{34}S_b$ isotope shift, but the 326-cm^{-1} band shows none, as expected for the noninteracting B_{3g}^t mode. Thus, the B_{3g}^t frequency is the same for sp fd as for $Fe_2S_2(S_2\text{-}o\text{-}xyl)_2^{2-}$. It seems reasonable that the A_g mode should likewise be at the same frequency, ~310 cm^{-1}, and that the 336-cm^{-1} sp fd RR band is the B_{1u}^t mode, 338 cm^{-1} (IR) in $Fe_2S_2(S_2\text{-}o\text{-}xyl)_2^{2-}$, its 2-$cm^{-1}$ $^{34}S_b$ shift arising from interaction with the B_{1u}^b mode. Activation of both B_{1u} modes in the protein RR spectra can occur by a common symmetry-lowering mechanism (vide infra). For ado, however, the 326-cm^{-1} band shows a 3-cm^{-1} $^{34}S_b$ shift, ruling out a B_{3g}^t (or B_{2u}^t) assignment. Instead, this mode is assigned to the 312-cm^{-1} band, which does not show a significant isotope shift. The $^{34}S_b$-sensitive 326- and 346-cm^{-1} bands are assigned to A_g^t and B_{1u}^t, respectively, both of them interacting with bridging modes of corresponding symmetry. Thus, the sp fd terminal mode frequencies match those of $Fe_2S_2(S_2\text{-}o\text{-}xyl)_2^{2-}$, but those of ado are shifted appreciably. The calculated terminal mode frequencies are in reasonable agreement with the assignments for $Fe_2S_2(S_2\text{-}o\text{-}xyl)_2^{2-}$ and sp fd.

Molecular and Electronic Structure. The sp fd RR spectrum is modeled quite well by $Fe_2S_2(S_2\text{-}o\text{-}xyl)_2^{2-}$. The bridging mode frequencies are somewhat higher in the proteins (by ~10 cm^{-1} for B_{3u}^b and B_{1u}^b and possibly by ~20 cm^{-1} for B_{2g}^b); apparently there are additional interactions at the protein site that tighten up the bridging structure. The terminal mode frequencies, however, are essentially the same for protein and analogue. This close agreement is in marked contrast to the situation encountered with rubredoxin and its analogue, $Fe(S_2\text{-}o\text{-}xyl)_2^{2-}$, which show substantially different Fe–S frequencies, attributable to ligand conformational differences.[20] Since there is no reason to think that such differences would not also be manifest for the 2Fe–2S complexes, we infer that the sp fd thiolate conformations are similar to those of $Fe_2S_2(S_2\text{-}o\text{-}xyl)_2^{2-}$. By extension, the marked differences in the ado terminal frequencies (10- and 16-cm^{-1} increases for B_{1u}^t and A_g^t; 14-cm^{-1} decrease for B_{3g}^t) may reflect a different set of cysteine conformations in this protein. The bridging frequencies, however, are nearly the same for ado and sp fd, implying very similar Fe_2S_2 structures.

A striking feature of the protein RR spectra is that the IR-active B_{1u} modes (284 and 336 cm^{-1} for sp fd; 289 and 346 cm^{-1} for ado) are as strong as, or stronger than, their A_g counterparts; the B_{3u} mode (424 and 419 cm^{-1}) also has appreciable RR intensity. Clearly there is a marked breaking of the nominal D_{2h} symmetry of the $Fe_2S_2(S\text{-}Cys)_4$ site in both proteins. Since the frequencies themselves are so similar to those of the analogue complexes (especially for sp fd), a significant distortion of the ground-state structure can be ruled out. Rather, a secondary interaction, affecting the excited state primarily, is implicated. The strong intensification of the B_{1u} modes implies an excited-state distortion involving these particular normal coordinates.[38] Since B_{1u} modes are polarized along the z (Fe–Fe) axis, an inequivalency of the two ends of the complex is indicated.

A charged group located closer to one Fe than the other, or H bonds directed at one of the two pairs of thiolate ligands, would provide the sort of interaction capable of inducing a z-directed distortion of the excited state, without appreciably altering the ground-state frequencies. There do not appear to be any charged groups close to the active site in the available crystal structure of fd from *Spirulina platensis*,[15] but there are several H bonds directed at the sulfur atoms, and it appears[15] that the cysteine sulfur atoms on one Fe, but not the other, have *two* H bonds each. This apparent increase in the H bonding at one end of the complex might account for the B_{1u} mode intensification.

It is of interest in this connection that in reduced 2Fe–2S proteins, the odd electron is localized on one of the two Fe ions, as revealed by Mössbauer spectroscopy.[7,9] Although there is recent evidence[40] that reduction of $Fe_2S_2(S_2\text{-}o\text{-}xyl)_2^{2-}$ also produces a trapped valence structure, it is possible that the protein asymmetry implied by the B_{1u} mode activation contributes to the electronic localization.

Reduced Adrenodoxin. Figure 5 shows the RR spectrum of reduced adrenodoxin with 5682-Å excitation, in resonance with a weak, but distinct, bump in the absorption spectrum, at ~550 nm (Figure 4). At other wavelengths we were unable to observe a spectrum. Also shown in Figure 5 is the RR spectrum of ado_{ox}, at the same wavelength. The ado_{ox} absorption spectrum also has a bump, of comparable intensity, at 550 nm; the absorptivity is much higher at shorter wavelengths than for ado_{red}. The ado_{red} RR spectrum has bands that correlate with the 289-, 391-, and 419-cm^{-1} bands of ado_{ox}, but they are down shifted by 16–24 cm^{-1}. (It is possible that the broad 395-cm^{-1} band of ado_{red} contains a contribution from the strong 391-cm^{-1} ado_{ox} band, due to incomplete reduction.) These are all bridging modes, and their lowered frequencies are consistent with the expected weakening of the bridge bonds upon reduction of one of the Fe^{III} ions to Fe^{II}. While the symmetry of a $Fe^{III}Fe^{II}S_2$ ring is lowered from D_{2h} to C_{2v}, the phasing of the Fe–S stretches in the various bridging modes (Figure 10) remains the same, and a general frequency lowering can be expected due to the aggregate lowering of the Fe^{III}–S + Fe^{II}–S force constants.

This argument does not apply, however, to the terminal modes. The terminal Fe–S stretches are not expected to couple significantly across the bridge, particularly for an unsymmetrical $Fe^{III}Fe^{II}S_2$ structure. Consequently, distinct Fe^{III}–S_t and Fe^{II}–S_t modes (in- and out-of-phase combinations) should exist, although the Fe^{II}–S modes are not expected to be resonance enhanced since $S \rightarrow Fe^{II}$ CT transitions occur in the ultraviolet. The Fe^{III}–S_t modes, however, should be enhanced, as they are in ado_{ox}. We are therefore puzzled at the absence of strong bands in the 300–350-cm^{-1} region. A weak band is observed at 308 cm^{-1}, and since ado_{ox} Fe–S_t bands are observed as low as 310 cm^{-1} (B_{3g}; see Figure 3), the 308-cm^{-1} band might arise from Fe^{III}–S_t stretching. A possible explanation for the weakness of the ado_{red} Fe^{III}–S_t modes is that the 550-nm absorption band is a low-energy $S_b \rightarrow Fe^{III}$ CT transition and that the Fe–S_t enhancement in ado_{ox} is due to somewhat higher lying $S_t \rightarrow Fe^{III}$ transitions, which are weaker in ado_{red}.

Raman Intensities and Excitation Profiles. The vis–UV absorption spectra of Fe_2S_2 complexes are broad and contain many overlapping bands due to CT transitions from both bridging S^{2-} and terminal RS^- ligands, which have not been specifically assigned. All five (half-filled) Fe^{3+} d orbitals are available as terminal orbitals for the CT transitions; they are expected to fall into two groups, d_σ and d_π, with a separation, 10 Dq, estimated to be ~10 000 cm^{-1} for tetrahedral Fe^{3+} in a sulfur environment. Each S^{2-} has four filled valence orbitals (s, p_x, p_y, p_z) available for CT transitions, while RS^- has three. The energies of these orbitals depend on the bonding interactions in the complex.

Figure 1 shows that bridging [393 (A_{1g}) and 284 (B_{1u}) cm^{-1}] and terminal [326 (B_{1u}) and 326 (B_{3g}) cm^{-1}] mode RR intensities have different wavelength dependences for sp fd. The bridging modes weaken more rapidly than the terminal modes as the laser is tuned to wavelengths longer than 500 nm. [Similar trends have been observed qualitatively for ado and for $Fe_2S_2(S_2\text{-}o\text{-}xyl)_2^{2-}$.] This differentiation suggests that $S_t \rightarrow$ Fe CT occurs near 520 nm while $S_b \rightarrow$ Fe CT occurs at ~450 nm. In addition, the 5682-Å RR spectrum of ado (Figure 5), showing more intense bridging than terminal modes, suggests another S_b–CT transition at ~570 nm. Thus, in the visible region it appears that a $S_t \rightarrow$

(40) Mascharak, P. K.; Papefthymiou, G. C.; Frankel, R. B.; Holm, R. H. *J. Am. Chem. Soc.* **1981**, *103*, 6110.
(41) Moss, T. H.; Petering, D.; Palmer, G. *J. Biol. Chem.* **1969**, *244*, 2275.
(42) Solomon, E. I.; Dooley, D. M.; Wang, R.-H.; Gray, H. B.; Cerdonio, M.; Magno, F.; Romani, G. L. *J. Am. Chem. Soc.* **1976**, *98*, 1029.
(43) Larrabee, J.; Spiro, T. G. *J. Am. Chem. Soc.* **1980**, *102*, 4217.
(44) Himmelwright, R. S.; Eickman, N. C.; Solomon, E. I. *Proc. Natl. Acad. Sci. U.S.A.* **1979**, *76*, 2094.

Fe CT band is flanked by $S_b \rightarrow$ Fe CT bands on either side. It seems likely that similar interleaving of $S_b \rightarrow$ Fe and $S_t \rightarrow$ Fe transitions continues into the UV.

In the case of $Fe_2S_2Cl_4^{2-}$, it is expected that the Cl → Fe CT transitions would be higher in energy than $S_t \rightarrow$ Fe CT transitions, because Cl^- has a higher electronegativity than RS^-. For $FeCl_4^-$, the lowest CT band is at 365 nm.[45] Consistent with this, we observed appreciable intensification of the Fe–Cl RR bands, relative to the Fe–S bands with 3638-Å Ar^+ excitation (not shown) in resonance with a strong absorption band[35] (357 nm) that is plausibly due to Cl → Fe CT. At this wavelength, the Fe–Cl A_g mode (318 cm^{-1}) is strong, while the B_{3g} mode (331 cm^{-1}) is weak. The reversal of this intensity pattern at 4545 Å (Figure 7) is interesting, since the B_{3g} mode must gain its intensity via a *B* term mechanism, involving vibronic mixing of two electronic transitions.[38] The symmetry of the mode (*yz*) requires that it mix a transition polarized along the Fe–Fe axis (*z*) with one perpendicular to the Fe_2S_2 plane (*y*). While both transitions could in principle involve Fe_2S_2 orbitals only, it seems more likely that the B_{3g} Fe–Cl mode mixes a resonant (at 4545 Å) *z*-polarized S → Fe CT transition (e.g., $S_{p_z} \rightarrow Fe_{d_{xz}}$) with a *y*-polarized Cl → Fe CT transition (e.g., $Cl_{p_z} \rightarrow Fe_{d_{yz}}$) at higher energy. A similar mechanism can account for the B_{3g} mode intensification for $Fe_2S_2(S_2\text{-}o\text{-xyl})_2^{2-}$, sp fd, and ado. It is interesting that the B_{2g} bridging mode is not similarly enhanced: the $Fe_2S_2Cl_4^{2-}$ RR spectrum is blank in the region (~360 cm^{-1}) where the B_{2g} mode is expected (Figure 7). This (*xz*) mode could analogously mix a *x*-polarized bridge transition (e.g., $S_{p_z} \rightarrow Fe_{d_{xz}}$) with a *z*-polarized terminal transition (e.g., $Cl_{p_y} \rightarrow Fe_{d_{yz}}$). It is possible, however, that these transitions are too far apart in energy for effective mixing. The B_{2g} bridging mode does show up with moderate intensity for sp fd (369 cm^{-1}) and weakly for ado (372 cm^{-1}). In the proteins, the same symmetry-breaking interaction responsible for the activation of the IR modes could provide an *A* term[38] mechanism for enhancement of the B_{2g} mode, which becomes totally symmetric as the molecular symmetry is lowered.

Fe–S Overtones, C–S Stretching, and Spin–Flip Transitions. Figure 6 shows the liquid N_2 RR spectrum of ado_{ox}, out to 1100 cm^{-1}. Beyond this, no additional Raman peaks could be detected above the slowly rising background. The low temperature sharpened up the spectrum and permitted the observation of a series of weak bands in the 550–800-cm^{-1} region, which can be identified with overtones and combinations of the Fe–S stretching modes, as shown in the figure. Similar overtone structure has been observed for rubredoxin and one-Fe analogue complexes.[20] In this region, the C–S stretching modes are also expected (there may be as many as four, associated with the four cysteine ligands, whose frequencies may vary, depending on the cysteine conformations), and they might be weakly enhanced via the S → Fe CT transitions.[20] There is a weak band at 622 cm^{-1} that does not line up with an overtone or combination level and is a candidate for C–S stretching. Another C–S mode may contribute to the relatively strong and broad band at 680 cm^{-1}.

Adar and co-workers[18,19] have drawn attention to the possibility of observing spin–flip transitions in the RR spectra of Fe_2S_2 proteins, in which the high-spin Fe ions are coupled antiferromagnetically, via the bridging sulfide ions, to give $S = 0$ ($S = {}^1/_2$ for the reduced forms) ground states. Adar et al.[18] reported a RR band of ado_{ox} at 995 cm^{-1} and assigned it to the $S = 0 \rightarrow 1$ transition, implying an exchange coupling constant, $-2J$, of the same magnitude. The protein is not detectably paramagnetic at room temperature,[6b] and $-2J$ has been estimated to be >700 cm^{-1}. Adar et al.[18] found another band at 2975 cm^{-1} and assigned it to $S = 0 \rightarrow 2$, expected at $-6J$. Our spectrum (Figure 6) shows what seems to be a very broad (~200 cm^{-1}) weak band, centered at ~1000 cm^{-1}, which might be the $S = 0 \rightarrow 1$ transition. (The width of the electronic level is difficult to predict; it depends on the zero-field splitting[18] and on the coupling to Fe–S vibrations.) It is much weaker and broader, however, than the band reported by Adar et al.[18]; their spectrum is of lower overall intensity (the Fe–S overtones do not appear in it), but the 995-cm^{-1} band is relatively prominent. We have been unable to observe their 2975-cm^{-1} band, and we believe that both of these bands were artifactual. The spectrum was obtained by irradiating a stationary liquid sample in a capillary tube. In our experience, this procedure can produce a coating of denatured protein on the capillary wall, at the laser focus, which gives rise to spurious Raman bands.

For sp fd_{ox} Blum et al.[19] reported the $S = 0 \rightarrow 1$ transition at 365 cm^{-1} in the RR spectrum, the position expected from the coupling constant determined from magnetic susceptibility measurements.[6b,41] However, as shown above, this band shifts on $^{34}S_b$ substitution and is therefore a Fe–S vibrational mode. Blum et al.[19] reported additional sp fd_{ox} bands at 1080 and 1930 cm^{-1} that they assigned to $S = 0 \rightarrow 2$ and 3 transitions (expected at ν 6*J* and 18*J*), and a pair of bands, at 770 and 1475 cm^{-1}, that appeared to lose intensity on cooling and were assigned to $S = 1 \rightarrow 2$ and 3 transitions. We have examined the sp fd_{ox} RR spectrum carefully and have observed weak overtone bands, including one at 785 cm^{-1} (2 × 391 cm^{-1}). However, none of the remaining bands, 1080, 1475, and 1930 cm^{-1}, reported by Blum et al. appeared in our spectrum, and we again attribute them to artifacts associated with laser-induced protein damage.

It is not unreasonable that spin–flip transitions might show up in RR spectra. Although these transitions are spin forbidden, they can acquire Raman intensity via resonance enhancement if there is an appreciable change in the spin–orbit coupling between the ground and excited state. In the case of oxyhemocyanin, which contains strongly spin-coupled Cu^{2+} ions and is diamagnetic at room temperature,[42] a broad RR band at 1075 cm^{-1} has been assigned to the $S = 0 \rightarrow 1$ transition.[43] It gains moderate intensity via resonance with an intense $O_2^{2-} \rightarrow Cu^{2+}$ CT transition at 345 nm.[44] The situation is not dissimilar in the Fe_2S_2 proteins, but at this point the evidence for spin–flip RR bands of these species is not persuasive.

Conclusions

(1) With the aid of ^{34}S substitution, IR as well as RR spectra of analogue complexes, and normal mode calculations, all of the Fe–S modes of 2Fe–2S proteins have been assigned. (2) The bridging Fe–S frequencies are similar for sp fd and ado, but the terminal frequencies show substantial differences, suggestive of altered conformations of the cysteine ligands. (3) Reduction of ado shifts the bridging frequencies down 16–24 cm^{-1}, consistent with weakening of the bridge bonds. The terminal modes lose enhancement. (4) A variety of RR enhancement mechanisms have been observed, including selective enhancement of bridging and terminal modes via $S_b \rightarrow$ Fe and $S_t \rightarrow$ Fe CT transitions, vibronic mixing, and activation due to symmetry lowering in the proteins. (5) The strong B_{1u} mode enhancement for both sp fd and ado implies an inequivalence of the two ends of the $Fe_2S_2(S\text{-Cys})_4$ complex, which is suggested to be due to stronger H bonding to the cysteine S atoms coordinated to one of the Fe atoms. (6) Previously reported RR bands of sp fd and ado that were assigned to spin–flip transitions of the coupled Fe ions have not been found and are believed to be artifactual. A weak and broad feature at ~1000 cm^{-1} in the ado RR spectrum might possibly be due to the $S = 0 \rightarrow 1$ transition.

Acknowledgment. This work was supported by National Institutes of Health Grant GM 13498 (to T.G.S.).

Registry No. $Fe_2S_2(S_2\text{-}o\text{-xyl})_2^{2-}$, 51203-73-7; $Fe_2S_2Cl_4^{2-}$, 62682-80-8.

(45) Czernuszewicz, R. S.; Johnson, M. K. *Appl. Spectrosc.* **1983**, *37*, 297.

^{17}O NMR Spectral Properties of Pyrophosphate, Simple Phosphonates, and Thiophosphate and Phosphonate Analogues of ATP

John A. Gerlt,*[1,2a] Mark A. Reynolds,[2b] Peter C. Demou,[2a] and George L. Kenyon[2b]

Contribution from the Department of Chemistry, Yale University, New Haven, Connecticut 06511, and the Department of Pharmaceutical Chemistry, School of Pharmacy, University of California, San Francisco, California 94143. *Received October 4, 1982*

Abstract: The chemical shifts of the ^{17}O resonances associated with the bridging and nonbridging oxygens of pyrophosphate have been unambiguously assigned; this information allows the assignment of the resonances of all of the phosphoryl oxygens of ADP and ATP. The chemical shifts of the phosphoryl oxygens in pyrophosphate and several nucleotide analogues with predictable proton ionization behavior, i.e., AMPS, ATPγS, methylphosphonate, methylenediphosphonate, and the β,γ-methylene analogue of ATP, have been measured as a function of pH; in each case an upfield change in chemical shift is observed upon protonation, with the magnitude of the shift change being approximately 50 ppm. These observations and those previously described (Gerlt, J. A.; Demou, P. C.; Mehdi, S. *J. Am. Chem. Soc.* **1982**, *104*, 2848) demonstrate that ^{17}O NMR spectroscopy can be used to quantitate the site and degree of charge neutralization in phosphate ester anions and related species.

Prior to 1980, the ^{17}O NMR spectral properties of the phosphoryl oxygens of inorganic and organic phosphates received little attention. However, in the past 3 years three research groups have published reports in this area.[3-7] This recent interest in the ^{17}O NMR properties of phosphates is largely the result of the recognition that ^{31}P NMR spectroscopy is unable to provide either qualitative or quantitative information about the sites and degree of charge neutralization of phosphate ester anions.[8] In biochemical systems, knowledge of the sites of coordination of nucleotides to protons, metal ions, and the cationic residues in the active sites of enzymes is essential to a complete understanding of many enyzmic reactions. Since coordination to the phosphate anions in nucleotides necessarily occurs by direct interaction with the phosphoryl oxygens, ^{17}O NMR spectroscopy should prove to be a useful spectroscopic technique for solving these types of problems. Although the ^{17}O NMR spectral properties of oxygen bonded to carbon and various metal nuclei have received considerable attention,[9,10] the advantages and limitations of ^{17}O NMR spectroscopy in the study of phosphates are yet to be fully defined.

With one exception, the recent ^{17}O NMR studies of phosphates have utilized regio- or stereospecifically enriched molecules, since these allow both convenient detection of resonances at concentrations useful in biochemical studies and also the ability to examine the properties of specific oxygens in nucleotides with more than one phosphoryl group, e.g., ATP. The natural abundance ^{17}O NMR study of several inorganic and organic phosphates was reported by Gerothanassis and Sheppard,[6] and the results these investigators reported are in excellent agreement with those obtained in Tsai's laboratory[3,5] and one of our own.[4,7]

In view of the limited information regarding the ^{17}O NMR properties of phosphates and phosphate esters and the incomplete understanding of the theory of ^{17}O NMR spectral parameters, one of our laboratories initiated a systematic investigation of the spectral properties of phosphate esters so that we could determine whether any useful empirical relationships exist between charge neutralization and spectral properties such as chemical shift. We recently reported the results of studies on the protonation of simple phosphate esters and the common adenine nucleotides.[7] Our data were uniformly consistent with the hypothesis that the magnitude of the charge located on a phosphoryl oxygen is a very important factor in determining the chemical shift of the associated ^{17}O NMR resonance: protonation of basic phosphoryl oxygens was observed to produce upfield chemical shifts of approximately 50 ppm per charge neutralized. Thus, even though the linewidths of the ^{17}O NMR resonances of phosphoryl oxygens can be relatively large (at least when compared to those of dipolar nuclei), charge neutralization can be easily detected and quantitated. This discovery that the chemical shift change induced by protonation is directly proportional to the magnitude of the charge neutralized suggests that ^{17}O NMR chemical shift information will be useful in solving otherwise difficult problems regarding charge neutralization of phosphate esters, e.g., proton binding to compounds with uncertain tautomeric structure and the ^{17}O NMR chemical shift changes that occur when divalent metal ions are added to samples of ADP and ATP.[5]

In this article we report additional ^{17}O NMR studies of biochemically important phosphates and phosphate analogues that are essential to further applications of this spectroscopic technique. We have determined the ^{17}O NMR spectral properties of samples of pyrophosphate with and without the bridging oxygen labeled. This information allows the resonances of oxygens in both environments to be assigned, thereby completing the assignments of all of the phosphoryl oxygens in ADP and ATP. More importantly, we have studied the ^{17}O NMR spectral properties of additional phosphorothioates and several phosphonates; the choice of compounds for study was based on two factors: (1) stable and predictable chemical structure and (2) the existence of anomalous ^{31}P NMR chemical shift behavior upon protonation. In all cases the ^{17}O NMR results confirmed our previous observation that protonation of basic phosphoryl oxygens induces upfield changes in chemical shift of approximately 50 ppm per charge neutralized.[7]

Materials and Methods

$H_2{}^{17}O$ (13% ^{16}O, 52% ^{17}O, and 35% ^{18}O) was purchased from Monsanto. Methylenediphosphonic acid (PCP), methylphosphonic acid, and thiophosphoryl chloride were obtained from Alfa. Unlabeled AMP and ADP and all enzymes were products of Sigma. All other chemicals used were the best grade commericially available and were used without further purification.

Nonbridging [$^{17}O_i$]Pyrophosphate. [α-$^{17}O_i$]ADP (containing ^{17}O only in the α-nonbridging oxygens) was prepared as previously described.[7] Oxidation of this material with periodate and subsequent base-catalyzed

(1) NIH Research Career Development Awardee (CA-00499), 1978–1983; Alfred P. Sloan Fellow, 1981–1983.
(2) (a) Yale University. (b) University of California.
(3) Tsai, M. D.; Huang, S. L.; Kozlowski, J. R.; Chang, C. C. *Biochemistry* **1980**, *19*, 3531.
(4) Coderre, J. A.; Mehdi, S.; Demou, P. C.; Weber, R.; Traficante, D. D.; Gerlt, J. A. *J. Am. Chem. Soc.* **1981**, *103*, 1870.
(5) Huang, S. L.; Tsai, M. D. *Biochemistry* **1982**, *21*, 951.
(6) Gerothanassis, I. P.; Sheppard, N. *J. Magn. Reson.* **1982**, *46*, 423.
(7) Gerlt, J. A.; Demou, P. C.; Mehdi, S. *J. Am. Chem. Soc.* **1982**, *104*, 2848.
(8) Jaffe, E. K.; Cohn, M. *Biochemistry* **1978**, *17*, 652.
(9) Klemperer, W. G. *Angew. Chem.* **1978**, *17*, 246.
(10) Harris, R. K. In "NMR and the Periodic Table"; Harris, R. K., Mann, B. E., Eds.; Academic Press: New York, 1978; Chapter 12.
(11) Richard, J. P.; Frey, P. A. *J. Am. Chem. Soc.* **1982**, *104*, 3476.

0002-7863/83/1505-6469$01.50/0